The Hexagonal Laves Phase $MgIr_2$

Viktor Hlukhyy and Rainer Pöttgen

Institut für Anorganische und Analytische Chemie,
Westfälische Wilhelms-Universität Münster,
Corrensstraße 36, D-48149 Münster (Germany)

Reprint requests to R. Pöttgen.
E-mail: pottgen@uni-muenster.de

The hexagonal Laves phase $MgIr_2$ was synthesized from the elements in a sealed tantalum tube in an induction furnace. $MgIr_2$ was investigated by powder and single crystal X-ray data: $P6_3/mmc$, $a = 516.9(1)$, $c = 838.5(2)$ pm, $wR2 = 0.0771$, 135 F^2 values, and 11 variable parameters. The magnesium atoms have coordination number (CN) 16 (12 Ir + 4 Mg), while the smaller iridium atoms, Ir1 and Ir2, both have CN 12 (6 Ir + 6 Mg). The Ir–Ir distances within the three-dimensional network of face- and corner-sharing $Ir_{4/2}$ tetrahedra range from 250 to 267 pm. The magnesium atoms have one shorter (306 pm) and three longer (319 pm) magnesium contacts. The crystal chemistry of $MgIr_2$ is briefly discussed and compared with the other binary Mg–Ir intermetallics.

Key words: Magnesium, Iridium, Crystal Structure,
Solid State Synthesis

Introduction

The binary system magnesium–iridium is characterized by the intermetallic compounds $Mg_{29}Ir_4$ (12.1 at.-% Ir) [1], $Mg_{44}Ir_7$ (13.7 at.-% Ir) [2, 3], $Mg_{13}Ir_3$ (18.8 at.-% Ir, formely reported with the approximate composition Mg_4Ir) [4, 5], Mg_3Ir (25 at.-% Ir) [6], Mg_5Ir_2 (28.6 at.-% Ir) [7], MgIr (50 at.-% Ir) [8], and $Mg_{2.30}Ir_{2.70}$ (54 at.-% Ir) [9]. Our recent phase analytical investigations in the iridium rich part of the phase diagram revealed the hexagonal Laves phase $MgIr_2$ as the so far most iridium rich compound. The synthesis and structure refinement of $MgIr_2$ are reported herein.

Experimental Section

Synthesis

Starting materials for the preparation of the $MgIr_2$ samples were a magnesium rod (Johnson Matthey, ∅ 16 mm,

Table 1. Crystal data and structure refinement for $MgIr_2$.

Empirical formula	$MgIr_2$
Formula weight	408.71 g/mol
Unit cell dimensions	$a = 516.9(1)$ pm
(Guinier data)	$c = 838.5(2)$ pm
	$V = 0.1940$ nm^3
Pearson symbol	hP12
Structure type	$MgZn_2$
Space group	$P6_3/mmc$
Formula units per cell	$Z = 4$
Calculated density	13.99 g/cm^3
Crystal size	$20 \times 30 \times 35$ μm^3
Transmission ratio (max/min)	12.91
Absorption coefficient	136.8 mm^{-1}
F (000)	664
Detector distance	60 mm
Exposure time	25 min
ω Range; increment	0 – 180°, 1.0°
Integration parameters A, B, EMS	13.5, 3.0, 0.010
θ Range for data collection	4° to 30°
Range in hkl	$\pm 7, \pm 7, \pm 11$
Total no. of reflections	1841
Independent reflections	135 ($R_{int} = 0.2723$)
Reflections with $I > 2\sigma(I)$	133 ($R_{sigma} = 0.0842$)
Data / restraints / parameters	135 / 0 / 11
Goodness-of-fit on F^2	1.274
Final R indices [$I > 2\sigma(I)$]	$R1 = 0.0394$; $wR2 = 0.0764$
R Indices (all data)	$R1 = 0.0403$; $wR2 = 0.0771$
Extinction coefficient	0.024(2)
Largest diff. peak and hole	3.18 and -3.61 e/Å^3

> 99.5%) and iridium powder (Degussa-Hüls, 200 mesh, > 99.9%). Pieces of the magnesium rod (the surface of the rod was first cut on a turning lathe in order to remove surface impurities) and a cold-pressed pellet of iridium (∅ 6 mm) were weighed in the atomic ratio 2Mg:3Ir and put in a glassy carbon crucible (SIGRADUR®G, type GAZ006). The latter was placed in a water-cooled sample chamber [10] of an induction furnace (Hüttinger Elektronik, Freiburg, Typ TIG 1.5/300). The mixture of the elements was first heated under flowing argon up to *ca.* 1300 K. The argon was purified over silica gel, molecular sieves, and titanium sponge (900 K). After the melting procedure the sample was cooled within 30 min to *ca.* 1200 K and held at that temperature for another 30 min. Then the sample was cooled within one hour to *ca.* 700 K and finally quenched by switching off the furnace. The light gray sample could easily be separated from the glassy carbon crucible. No reactions whatsoever with the crucible material could be detected.

The X-ray powder patterns of this sample showed MgIr [8] and iridium as reaction products. The inductively melted ingot was then ground to powder in a steel mortar, cold-pressed to a pellet of 6 mm diameter and placed in a tantalum tube. This tube was first heated to *ca.* 1400 K, cooled

Atom	Wyckoff position	x	y	z	U_{11}	U_{22}	U_{33}	U_{12}	U_{eq}
Mg	4f	1/3	2/3	0.068(1)	75(30)	U_{11}	119(45)	38(15)	90(21)
Ir1	2a	0	0	0	62(7)	U_{11}	114(8)	31(4)	79(6)
Ir2	6h	0.82807(9)	2×	1/4	54(6)	35(6)	128(6)	18(3)	74(5)

Table 2. Atomic coordinates and anisotropic displacement parameters (pm^2) for $MgIr_2$. U_{eq} is defined as one third of the trace of the orthogonalized U_{ij} tensor. $U_{13} = U_{23} = 0$.

to *ca.* 1300 K within 30 min, kept at that temperature for another 30 min, cooled to 700 K within one hour and finally quenched to room temperature. The sample is stable in air as a compact button as well as a fine-grained powder. Single crystals exhibit metallic luster.

The $MgIr_2$ single crystal investigated on the imaging plate diffractometer and the bulk sample have been analyzed by an EDX measurement using a LEICA 420 I scanning electron microscope with MgO and iridium as standards. No impurity elements were detected. The analyses 33 ± 2 at.-% Mg : 67 ± 2 at.-% Ir are in excellent agreement with the ideal composition of 33.3 at.-% Mg : 66.7 at.-% Ir.

X-ray film data and structure refinement

The $MgIr_2$ sample was characterized through its Guinier powder pattern using Cu-K$_{\alpha_1}$ radiation and α-quartz ($a = 491.30$, $c = 540.46$ pm) as an internal standard. The Guinier camera was equipped with an image plate system (Fujifilm BAS–1800). The indexing of the powder data was facilitated by an intensity calculation [11] using the atomic parameters of the refined structure. The hexagonal lattice parameters (Table 1) were obtained by least-squares fits of the Guinier data.

Irregularly-shaped single crystals were isolated from the annealed sample by mechanical fragmentation and examined on a Buerger precession camera (equipped with an imaging plate system Fujifilm BAS–1800) in order to establish suitability for intensity data collection. Single crystal intensity data were collected at room temperature on a Stoe IPDS–II diffractometer with graphite monochromatized Mo-K$_\alpha$ radiation. All relevant crystallographic data for the data collection and evaluation are listed in Table 1.

The isotypism of $MgIr_2$ with the hexagonal Laves phase was already evident from the X-ray powder data. The atomic positions of the prototype $MgZn_2$ [12] were taken as starting values and the structure was refined using SHELXL-97 (full-matrix least-squares on F_o^2) [13] with anisotropic atomic displacement parameters for all sites. As a check for the correct composition, the occupancy parameters were refined in a separate series of least-squares cycles. The occupancy parameters varied between 99(1)% for Ir2 and 103(7)% for Mg. Thus, all sites were fully occupied within one standard deviation. In the last cycles, the ideal occupancies were assumed again. A final difference Fourier synthesis revealed no significant residual peaks (see Table 1). The highest residual peaks were all close to the iridium sites (137 pm to Ir2) and most likely resulted from an incomplete absorption correction of

Table 3. Interatomic distances (pm) of $MgIr_2$ (standard deviations in parentheses), calculated with the powder lattice parameters.

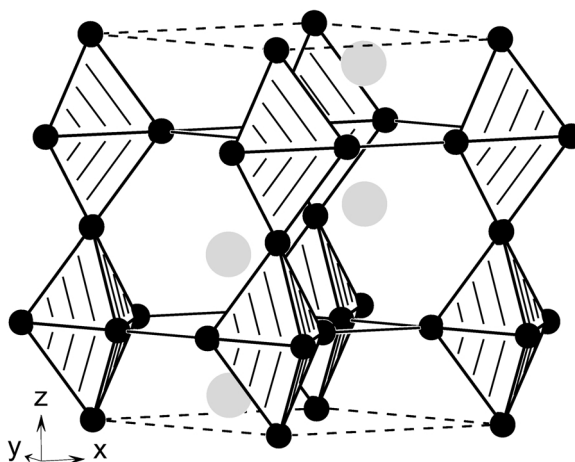| Mg:	6	Ir2	300.3(6)	Ir1:	6	Ir2	260.1(1)
	3	Ir2	303(1)		6	Mg	303.8(2)
	3	Ir1	303.8(2)	Ir2:	2	Ir2	250.3(1)
	1	Mg	306(2)		2	Ir1	260.1(1)
	3	Mg	319.3(8)		2	Ir2	266.6(2)
					4	Mg	300.3(6)
					2	Mg	303(1)

Fig. 1. The crystal structure of $MgIr_2$. Large gray and small filled circles represent magnesium and iridium, respectively. The three-dimensional network of face- and corner-sharing $Ir_{4/2}$ tetrahedra is emphasized.

this highly absorbing compound. The positional parameters and interatomic distances are listed in Tables 2 and 3. Further details on the structure refinement are available.*

Discussion

$MgIr_2$ crystallizes with the structure of the hexagonal Laves phase $MgZn_2$ [12] (Fig. 1). As emphasized in the Figure, the Ir1 and Ir2 atoms build up rows of face- and corner-sharing $Ir_{4/2}$ tetrahedra along the c axis. These are connected *via* Ir–Ir bonds within the *ab* planes at $z = 1/4$ and $z = 3/4$ forming a three-
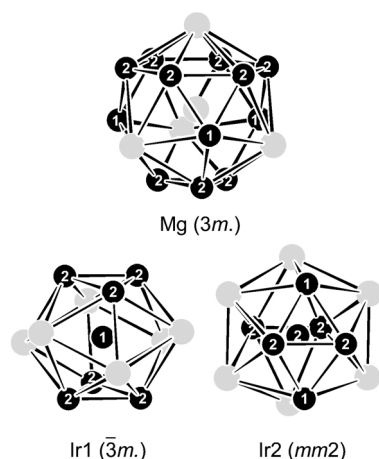
Fig. 2. Coordination polyhedra in the $MgIr_2$ structure. Large gray and small filled circles represent magnesium and iridium, respectively. Atom designations and site symmetries are indicated.

dimensional network. The Ir–Ir distances within the tetrahedral network range from 250 to 267 pm. These Ir–Ir distances are all shorter than in *fcc* iridium [14] where each iridium atom has twelve iridium neighbors at 272 pm. Even shorter Ir–Ir distances occur in the complex structures of $Mg_{2.30}Ir_{2.70}$ [9] (245 and 258 pm) and MgIr [8] (245–266 pm). Thus, Ir–Ir bonding plays certainly an important role in this Laves phase. The Mg–Ir distances (300–304 pm), on the other hand, are significantly longer than the sum of the covalent radii of 262 pm for iridium and magnesium [15]. Each magnesium atom in $MgIr_2$ has four nearest magnesium neighbors at Mg–Mg distances of 306 and 319 pm. These compare well with the average Mg–Mg distance of 320 pm in *hcp* magnesium [14].

The coordination polyhedra of the $MgIr_2$ structure are shown in Fig. 2. The magnesium atoms have (CN) 16 (12 Ir + 4 Mg), while the smaller iridium atoms, Ir1 and Ir2, both have CN 12 (6 Ir + 6 Mg). The 12 neighbors around the Ir1 and Ir2 sites have slightly distorted icosahedral arrangements. The three different coordination polyhedra in the $MgIr_2$ structure are slightly distorted Frank-Kasper polyhedra [16, 17]. At this point it is interesting to note, that the structure of $Mg_{2.30}Ir_{2.70}$ [9], with a slightly smaller iridium content, contains slabs of the $MgIr_2$ structure.

Laves phases can adopt three different structures, *i.e.* the cubic $MgCu_2$ or the hexagonal $MgZn_2$ and $MgNi_2$ types [18–21, and ref. therein]. Which type occurs depends on electronic as well as on geometrical features. Johnston and Hoffmann [20] have investigated the structure–bonding relationships in Laves phases by performing extended Hückel band structure calculations. These studies revealed that the type of the Laves phase depends on the valence electron concentration (VEC). The AIr_2 Laves phases with $A =$ alkaline earth and rare earth metals, Zr, Th, U, and Np [22–24] crystallize all with the cubic $MgCu_2$ type structure. The cubic AIr_2 compounds with a divalent A component have all 20 valence electrons per formula unit. According to the diagrams of Johnston and Hoffmann [20], the compounds with VEC = 20 are at the border between the hexagonal and the cubic network. For $MgIr_2$ described herein, the much smaller size of magnesium seems to favor the hexagonal $MgZn_2$ type.

[1] F. Bonhomme, K. Yvon, J. Alloys Compd. **227**, L1 (1995).

[2] L. Westin, Chemica Scripta **1**, 127 (1971).

[3] L. Westin, L.-E. Edshammar, Acta Chem. Scand. **26**, 3619 (1972).

[4] R. Ferro, G. Rambaldi, R. Capelli, J. Less-Common Met. **4**, 16 (1962).

[5] V. Hlukhyy, U.Ch. Rodewald, R.-D. Hoffmann, R. Pöttgen, Z. Naturforsch. **59b**, 251 (2004).

[6] K.-J. Range, P. Hafner, J. Alloys Compd. **191**, L5 (1993).

[7] R. Černý, J.-M. Joubert, H. Kohlmann, K. Yvon, J. Alloys Compd. **340**, 180 (2002).

[8] R. Černý, G. Renaudin, V. Favre-Nicolin, V. Hlukhyy, R. Pöttgen, Acta Crystallogr. B **60**, 272 (2004).

[9] V. Hlukhyy, R. Pöttgen, Solid State Sci., submitted.

[10] D. Kußmann, R.-D. Hoffmann, R. Pöttgen, Z. Anorg. Allg. Chem. **624**, 1727 (1998).

[11] K. Yvon, W. Jeitschko, E. Parthé, J. Appl. Crystallogr. **10**, 73 (1977).

[12] J. B. Friauf, Phys. Rev. **29**, 35 (1927).

[13] G. M. Sheldrick, SHELXL-97, Program for Crystal Structure Refinement, University of Göttingen, Germany (1997).

[14] J. Donohue, "The Structures of the Elements", Wiley, New York (1974).

[15] J. Emsley, The Elements, Oxford University Press, Oxford (1999).

[16] F. C. Frank, J. S. Kasper, Acta Crystallogr. **11**, 184 (1958).

[17] F. C. Frank, J. S. Kasper, Acta Crystallogr. **12**, 483 (1959).

[18] A. Simon, Angew. Chem. **95**, 94 (1983).

[19] R. Nesper, Angew. Chem. **103**, 805 (1991).

[20] R. L. Johnston, R. Hoffmann, Z. Anorg. Allg. Chem. **616**, 105 (1992).

[21] R. Nesper, G. J. Miller, J. Alloys Compd. **197**, 109 (1993).

[22] E. A. Wood, V. B. Compton, Acta Crystallogr. **11**, 429 (1958).

[23] R. Pöttgen, R.-D. Hoffmann, M. H. Möller, G. Kotzyba, G. Künnen, C. Rosenhahn, B. D. Mosel, J. Solid State Chem. **145**, 174 (1999).

[24] P. Villars, L. D. Calvert, Pearson's Handbook of Crystallographic Data for Intermetallic Phases, Second Edition, American Society for Metals, Materials Park, OH 44073 (1991), and desk edition (1997).